Hydration Numbers of Biologically Relevant Divalent Metal Cations from *Ab Initio* Molecular Dynamics and Continuum Solvation Methods

Tadeáš Kalvoda, Tomas Martinek, Pavel Jungwirth, Lubomír Rulíšek*

Institute of Organic Chemistry and Biochemistry of the Czech Academy of Sciences, Flemingovo nám. 2, 160 00 Praha 6, Czechia, Contact email: lubomir.rulisek@uochb.cas.cz

Abstract

Hydration and, in particular, coordination number (CN) of a metal ion, is of paramount importance as it defines many of its (bio)physico-chemical properties. It is not only essential for understanding its behavior in aqueous solutions but also determines the metal-ion reference state and its binding energy to (bio)molecules. For the following divalent metal cations — Ca^{2+}, Cd^{2+}, Cu^{2+}, Fe^{2+}, Hg^{2+}, Mg^{2+}, Ni^{2+}, Pb^{2+}, and Zn^{2+} — we compare here two approaches for predicting hydration numbers: (1) a mixed explicit/continuum DFT-D3//COSMO-RS solvation model and (2) DFT-based *ab initio* molecular dynamics (AIMD). The former approach is employed to calculate Gibbs free energy change for the sequential hydration reactions, starting from $[M(H_2O)_2]^{2+}$ aqua complexes up to $[M(H_2O)_9]^{2+}$ allowing explicit water molecules to bind in the first or second coordination sphere and determining the most stable $[M(H_2O)_n]^{2+}$ structure. In the latter approach, the hydration number is obtained by integrating the ion-water radial distribution function. With a couple of exceptions, the metal ion hydration numbers predicted by the two approaches are in mutual agreement, as well as in agreement with the experimental data.

I.   Introduction

Metal dications play an important role in chemistry and biology. Their interactions with biomolecules impact fundamental processes ranging from protein folding and cellular communication to catalysis.[1] A reliable theoretical description of such interactions is crucial for metalloprotein design, protein structure prediction, metal binding affinity, etc.[2] From a physico-chemical view, most of these properties result from the equilibrium between the fully hydrated metal ion and its (partially dehydrated) bound state in the biomolecular complex. For example, the complexation constant of the metal ion in a particular complex with the ligand L (L is assumed to be neutral in Eq. 1 below, but can be of any charge, as in our previous work[3–6]) can be determined as the free energy change of the reaction:

$$[M(H_2O)_n]^{2+} + L \rightarrow [M(L)(H_2O)_m]^{2+} + (n - m)H_2O \qquad (1)$$
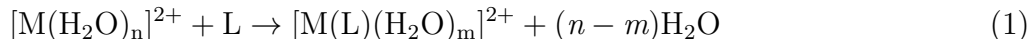
To predict such properties, both in absolute and relative scales (e.g., comparing binding energies of various metal ions in a particular site), the control over the l.h.s. of the Eq. 1 defining the reference state of the metal ion is essential. Indeed, an incorrect solvation state of the metal ion may affect the computed complexation free energies by several $kcal \cdot mol^{-1}$ leading to errors of a few orders of magnitude in the predicted equilibrium constants.[6] Over the last couple of decades, the hydration of metal ions has been studied both computationally and experimentally

as summarized in the following reviews.[7–9] There is a number of experimental techniques that provide information about the nature of the coordination of water molecules to a metal ion. These include, among others, neutron diffraction, nuclear magnetic resonance (NMR), X-ray crystallography, X-ray absorption near edge structure (XANES), and extended X-ray absorption fine structure (EXAFS).[10–14] At the same time, there are limitations involved, e.g., there may be cases where multiple semi-stable aqua complexes of ions are present, with the experimental techniques providing only averaged values.[15] Thus, complementary information provided by molecular level calculations is often essential to obtain a detailed understanding of the hydration phenomenon.

For most of the common metal dications (including Ca^{2+}, Cd^{2+}, Cu^{2+}, Fe^{2+}, Hg^{2+}, Mg^{2+}, Ni^{2+}, Pb^{2+}, and Zn^{2+}), the coordination number and geometry of each aqua complex have been examined by the experimental techniques mentioned above[7–9, 16–34] (see also Table I). For most of these ions, general consensus has been reached concerning coordination numbers and hydration shell geometries. CN of 6 with octahedral geometry of the first solvent shell is presumably adopted by Cd^{2+}, Fe^{2+}, Hg^{2+}, Mg^{2+}, Ni^{2+}, and Zn^{2+} ions[7–9, 17, 19, 23, 28, 32]. CN 5 with tetragonal pyramidal or trigonal bipyramidal coordination is observed for Cu^{2+} ion.[34] The situation is somewhat less clear for Ca^{2+}, where CNs of 6, 7, or 8 or even larger were reported.[7, 9, 16, 26] The geometry of the hexa-coordinated calcium ion is believed to be a regular octahedron, whereas it is probably prismatic for CN of 8.[16, 26, 29, 30] What remains rather unclear is the coordination number and hydration shell geometry of the Pb^{2+}. In an NMR study, CN of 6 has been reported,[27] whereas in other two experimental studies, CNs of 5–7 were proposed.[24, 25]

In this work, we aim to determine the coordination numbers of nine divalent cations by comparing two complementary theoretical approaches: a mixed explicit/continuum DFT-D3//COSMO-RS calculation and *ab initio* molecular dynamics (AIMD). The former approach is based on calculations of the free energy changes accompanying sequential hydrations, that is addition of a water molecule to the first or second coordination spheres of the $[M(H_2O)_n]^{2+}$ complex to form $[M(H_2O)_{(n+1)}]^{2+}$ complex (up to $n = 8$). For a perfect implicit solvation model this free energy change should equal to zero. However, sequential solvation of "naked" or only partially coordinated transition metal ions is described only approximately by implicit solvation models (including COSMO-RS), which were parameterized on bulk properties. What we actually observe is that the free energy changes are negative up to a certain CN_{opt}, becoming positive for $n > CN_{opt}$. Heuristically, we associate this sign change with the completion of the first hydration shell, with agreement between experimental and present AIMD data verifying this conjecture *a posteriori*.

Among the investigated metal dications, there are two examples of rare earth metals (Ca^{2+} and Mg^{2+}), three representatives of open-shell d-block elements (Cu^{2+}, Fe^{2+}, Ni^{2+}), three examples of their closed-shell counterparts (Zn^{2+}, Cd^{2+}, Hg^{2+}), and one p-block element (Pb^{2+}). Most of these divalent ions are commonly found to interact with biomolecules, through for Pb and Hg these are rather undesired interactions.[35, 36] At the same time, the selected metal ions represent both cases where the CN is well known (thus, it can be used for method calibration) and situations where controversies and ambiguities persist and where the present work may help to more firmly establish the coordination numbers.

TABLE I: Experimentally obtained coordination numbers and geometries for metal ions. If there are multiple coordination numbers in the published literature, all of them are listed. Results that were obtained significantly less frequently than the rest are listed in brackets.

M^{2+}	Experimental CN	Experimental geometry	Ref.
Ca^{2+}	6–8 (10)	Octahedron, Not determined	[16, 26, 29–31]
Cd^{2+}	6 (7)	Octahedron	[7, 32, 33]
Cu^{2+}	5	Tetragonal pyramid, Trigonal bipyramid	[7, 34]
Fe^{2+}	6	Octahedron	[7, 8, 17, 18]
Hg^{2+}	6 (7)	Octahedron, Irregular	[19–21]
Mg^{2+}	6	Octahedron	[7, 8]
Ni^{2+}	6	Octahedron	[22, 23]
Pb^{2+}	5–7	Not determined	[24, 25, 27]
Zn^{2+}	6	Octahedron	[7, 8, 22, 28]

II. Methods

A. Force field (classical) molecular dynamics

For the preparatory stage, we employed classical force field molecular dynamics simulations. The simulated systems consisted of a single metal cation (Ca^{2+}, Cd^{2+}, Cu^{2+}, Fe^{2+}, Hg^{2+}, Mg^{2+}, Ni^{2+}, Pb^{2+}, or Zn^{2+}) and 64 water molecules in a cubic simulation cell under periodic boundary conditions to mimic bulk solutions. No counterions were considered, therefore, the net charge of the system was 2+. The unit cell volume was set as the experimental volume of 64 water molecules plus the standard partial volume of the specific ion.[37] Because of the slow convergence of the volume of the system at constant pressure, especially in subsequent AIMD simulations, we carried out simulations in a canonical (constant volume and temperature) ensemble at 300 K. After equilibration, snapshots taken at intervals of 4 ns were used as the initial structures for subsequent AIMD simulations. Force field simulations were done using the CHARMM27 force field[38] with a rigid SPCE water model[39, 40] and ion parameterization taken from Ref. [41]. All force field simulations were performed using Gromacs, version 2021.1.[42]

B. *Ab initio* molecular dynamics

AIMD simulations within the Born–Oppenheimer approximation were performed employing the CP2K program package, version 9.1, using the Quickstep module.[43] The electronic structure of the system was described at the DFT level of theory employing the PBE functional[44], with D3

dispersion correction[45] and TZV2P MOLOPT basis set[46] for all atoms, with Goedecker–Teter–Hutter (GTH) effective core potentials[47] for water oxygens and for metal ions (see Table S1 in SI for metal ions; six explicit electrons were used for oxygen). For the equilibration, four independent trajectories were propagated for at least 3 ps, with a time step of 0.5 fs, NVT ensemble, $T = 298$ K, massive canonical sampling through velocity rescaling (CSVR) thermostat[48] with the time constant of 50 fs, and periodic boundary conditions. Next, we ran 80 ps long production simulations with the same settings and a global CSVR thermostat with a time constant of 1 ps. For each ion, we then combined all four trajectories to calculate the single radial distribution function (RDF). The coordination number was then calculated as the integral of the RDF from zero to its first minimum after the first peak.

C.   DFT calculations in implicit solvent

For each metal ion, eight initial structures were created, placing 2–9 water molecules in its first solvation shell, symmetrically whenever possible. Geometries of all structures were optimized employing the BP86 functional[49, 50] with D3 dispersion correction with Becke–Johnson damping[45, 51] and the def2-TZVP basis set. For Cd, Hg, and Pb, the Stuttgart–Dresden effective core potentials (ECP; $N_{core} = 28, 60, 60$) were used. COSMO solvation model was employed as an implicit solvent with the dielectric constant of $\epsilon_r = 80$ corresponding to water.[52] For the ionic radii for COSMO, we choose the ionic radii published by Shannon and coworkers,[53] scaled to the COSMO radii of $Zn^{2+} = 2.00$ Å, used in our previous work[3–5] and summarized in Table S2 in SI. All DFT calculations were carried out using the Turbomole 7.6 program.[54] Vibrational frequency calculations were performed *in vacuo*, at the same level of theory for all calculated structures on *in vacuo* reoptimized geometry. For all structures, we checked that the *in vacuo* minima do not significantly deviate from their solvent counterparts. As in previous work,[6] the free energy value corresponding to a particular structure can be expressed as:

$$G_{TOT} = E_{EL} + G_{SOLV} + E_{ZPVE} - RT \ln(q_{trans}q_{vib}q_{rot}) + pV \tag{2}$$

where E_{EL} is the electronic energy of the molecule *in vacuo* (gas-phase electronic energy), calculated with def2-TZVPD basis set, and the functional BP86-D3(BJ), G_{SOLV} is the solvation energy calculated by employing the COSMO-RS method (see below), E_{ZPVE} is the zero-point vibrational energy. The term $RT \ln(q_{trans}q_{rot}q_{vib})$ is the entropic correction obtained from the rigid-rotor/harmonic-oscillator (RRHO) approximation in which a free rotor model was applied for low-lying vibrational modes under 100 cm^{-1} with a smoothing function applied (sometimes denoted as quasi-RRHO, or RRFRHO approximation). The E_{EL} and $(E_{ZPVE} - RT \ln(q_{trans}q_{rot}q_{vib}) + pV)$ are calculated for equilibrium structures *in vacuo*.

The G_{SOLV} was obtained using Klamt's conductor-like screening model for the realistic solvation method (COSMO-RS).[55, 56] COSMO-RS calculations were carried out using COSMOtherm21 software[57] with the recommended protocol: BP86-D3(BJ)/def2-TZVPD single point calculations *in vacuo* on top of the *in vacuo* geometries and in an ideal conductor ($\epsilon = \infty$) for the optimized geometry in solvent, followed by the COSMO-RS calculations in water. FINE cavities were used to increase numerical precision.[58] Finally, a correction of $1.9 \cdot \Delta n$ kcal·mol^{-1} (corresponding to the difference between the concentration of the ideal gas at 298 K and 1 atm and its 1 mol·L^{-1} concentration; Δn is the change in the number of moles in the reaction) has been applied in order that the computed values refer to 1 mol·L^{-1} standard state. The following definition of the hydration Gibbs free energy, ΔG_{HYD} has been used throughout:

$$\Delta G_{\mathrm{HYD}} = G_{\mathrm{TOT}}(\text{products}) - G_{\mathrm{TOT}}(\text{reactants}) \qquad (3)$$

where products and reactants correspond to the r.h.s. and l.h.s., respectively, of the reaction:

$$[\mathrm{M(H_2O)_n}]^{2+} + \mathrm{H_2O} \rightarrow [\mathrm{M(H_2O)_{n+1}}]^{2+} \qquad (4)$$
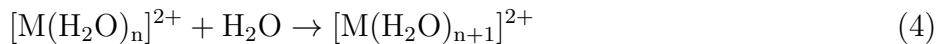
where n denotes the number of water molecules (2–9 water molecules, therefore $n = 2$–8 in Eq 4). We previously used an analogous approach in our peptide metal-binding studies, and it has been shown to provide quantitatively accurate data (wrt to the experimental isothermal calorimetry, ITC data).[3–5] In this approach, we presume that the coordination number can be associated with the structure for which the last sequential hydration reaction where ΔG is negative. As mentioned above, this assumption needs to be verified *a posteriori* by comparison with AIMD, and experiments (*cf.* Results and Discussion).

To further elaborate on this issue which concerns the applicability and limitations of continuum solvation models and the combination of explicit with implicit solvation models (the latter represented in this work by the COSMO and COSMO-RS), we also calculated the ΔG of addition of one water molecule to the water cluster (using the same DFT-D3//COSMO-RS protocol described above; see Table S3 and Chapter 3 in SI). This serves as the reference for the performance of the continuum models at the interface between explicit and implicit solvation.

III. Results and Discussion

First, we predict the optimal hydration number of all nine metal ions (Ca^{2+}, Cd^{2+}, Cu^{2+}, Fe^{2+}, Hg^{2+}, Mg^{2+}, Ni^{2+}, Pb^{2+}, and Zn^{2+}) employing the DFT-D3//COSMO-RS "sequential hydration" approach described above. In Table II, the ΔG values for the sequential water additions for all ions are listed. The DFT-D3//COSMO-RS optimal hydration number is assumed to be the CN associated with the last step with negative ΔG. The corresponding equilibrium geometries are then depicted in Fig. 1. The negative ΔG may be associated with the inherently imperfect implicit solvent model, such as COSMO-RS not being able to fully capture hydration in the immediate vicinity of a metal ion, i.e., in its first solvation sphere. After exceeding the optimal number of water molecules in the first solvation sphere, the additional water would end up in the second solvation shell. Here, the replacement of the implicit water with the explicit one should, in principle, be associated with zero ΔG. From Table II, we see that this is not the case with ΔG acquiring small positive values. Notably, these ΔG values for implicit/explicit water exchange are rather similar to those calculated for implicit/explicit water exchange in small water clusters (as described in Chapter 3 and Table S3 in the SI). Noteworthy, for some cations, the first unfavorable hydration reaction (with the positive ΔG) is associated with a rather small barrier (the value of ΔG of $\sim$1 kcal·mol^{-1} or smaller), and therefore we expect multiple aqua complexes that may exist in equilibrium.

TABLE II: ΔG of water addition (see equation 4) for all nine ions obtained with DFT-D3//COSMO-RS. The product of the last reaction with negative ΔG is the expected coordination number. All values are in $kcal \cdot mol^{-1}$. The last negative ΔG is highlighted.

$n \to n+1$	Ca^{2+}	Cd^{2+}	Cu^{2+}	Fe^{2+}	Hg^{2+}	Mg^{2+}	Ni^{2+}	Pb^{2+}	Zn^{2+}
$2 \to 3$	-22.9	-22.0	-31.3	-24.4	-13.8	-22.3	-26.3	-23.49	-24.27
$3 \to 4$	-16.3	-15.5	-18.0	-17.4	-10.5	-16.5	-20.0	-9.1	-16.4
$4 \to 5$	-8.0	-6.1	**-2.9**	-8.4	**-4.5**	-6.9	-11.1	**-3.7**	-3.6
$5 \to 6$	**-5.3**	**-3.3**[a]	2.4[a]	**-1.5**[a]	0.1[a]	**-4.9**[a]	**-6.5**[a]	2.6	**-2.0**[a]
$6 \to 7$	1.1	4.9	3.5	3.4	3.7	3.6	3.2	8.0	4.6
$7 \to 8$	6.4[a]	3.6	3.3	4.2	2.1	4.4	4.6	1.4[a]	3.0
$8 \to 9$	4.6	2.8	4.6	3.9	4.2	3.8	5.6	5.5	5.6

[a] These are the last aqua complexes where all explicit water molecules stay in the first solvation shell.
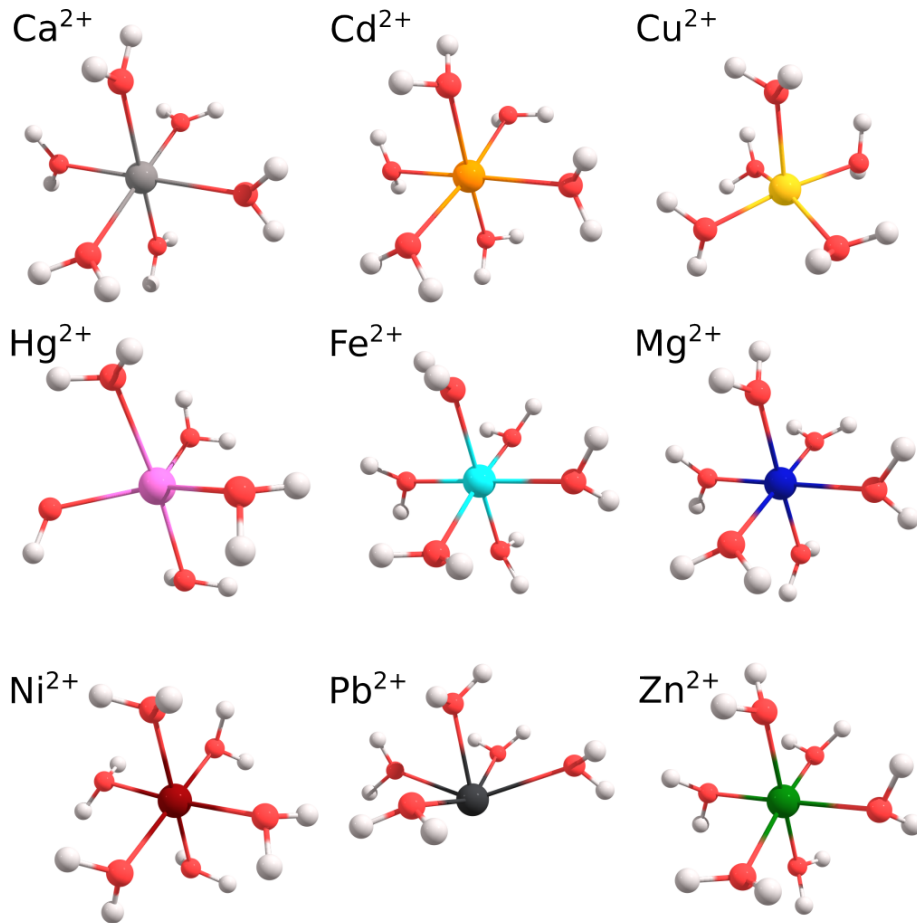
FIG. 1: DFT-D3//COSMO-RS equilibrium structures of all nine metal ions displaying their preferred hydration number.

Next, we investigate the hydration structures of the metal dications using AIMD simulations. From the obtained trajectories, we calculate radial distribution functions (RDFs) with the first peaks corresponding to the optimal M^{2+}–O distances ($\sim$2.0 Å for Cu^{2+}, Fe^{2+}, Mg^{2+}, Zn^{2+}, and Zn^{2+}, $\sim$2.4 Å for Ca^{2+}, Cd^{2+}, and Hg^{2+}, and $\sim$2.6 Å for Pb^{2+}), as depicted in Fig. 2. These maxima of the first RDF peaks loosely correlate with the ionic radii. It is worth noticing that peaks of RDFs of some of the ions like Cu^{2+} and Hg^{2+} are asymmetric, suggesting the broken symmetry of their solvation shell. Comparing the RDF peak positions with M^{2+}–O distances from DFT-D3//COSMO-RS optimized structures (Table III), the AIMD distances are, in general, slightly larger. This may be the effect of the stronger hydrogen bonding to higher solvation layers, which are treated only implicitly in the COSMO and COSMO-RS solvation models, and possibly also the effect of temperature fluctuations in the AIMD simulation.

It is also important to note that the dispersion interaction D3 coefficients were parameterized for neutral atoms, and it was shown previously that turning it off for the metal ion may lead to slightly different M^{2+}–O distances.[59] In most cases, the difference between DFT-D3//COSMO-RS and AIMD distances is $\sim$0.03 Å, which is considered as a good agreement. An exception is Zn^{2+}, suggesting a different coordination number between AIMD and the DFT-D3//COSMO-RS, as discussed later. For Pb^{2+}, there are five distinct Pb^{2+}–O distances, all of them shorter than the peak position from AIMD, in line with previous reasoning. Significantly broad RDF peak for Pb^{2+} is pointing to multiple different distances as well in AIMD, and therefore, either to its

irregular first solvation shell or multiple stable configurations. This may originate from the uneven, "hemidirected" hydration assumed for aqua complexes of Pb^{2+} with up to 6 or 7 waters. Finally, experimental distances (obtained mostly with X-ray diffraction, neutron scattering, XANES, and EXAFS) are in agreement with the present calculations, typically within a few hundredths of Å (Table III). Notably, all six of the bond lengths for Pb^{2+} are within the spread of the experimental values.
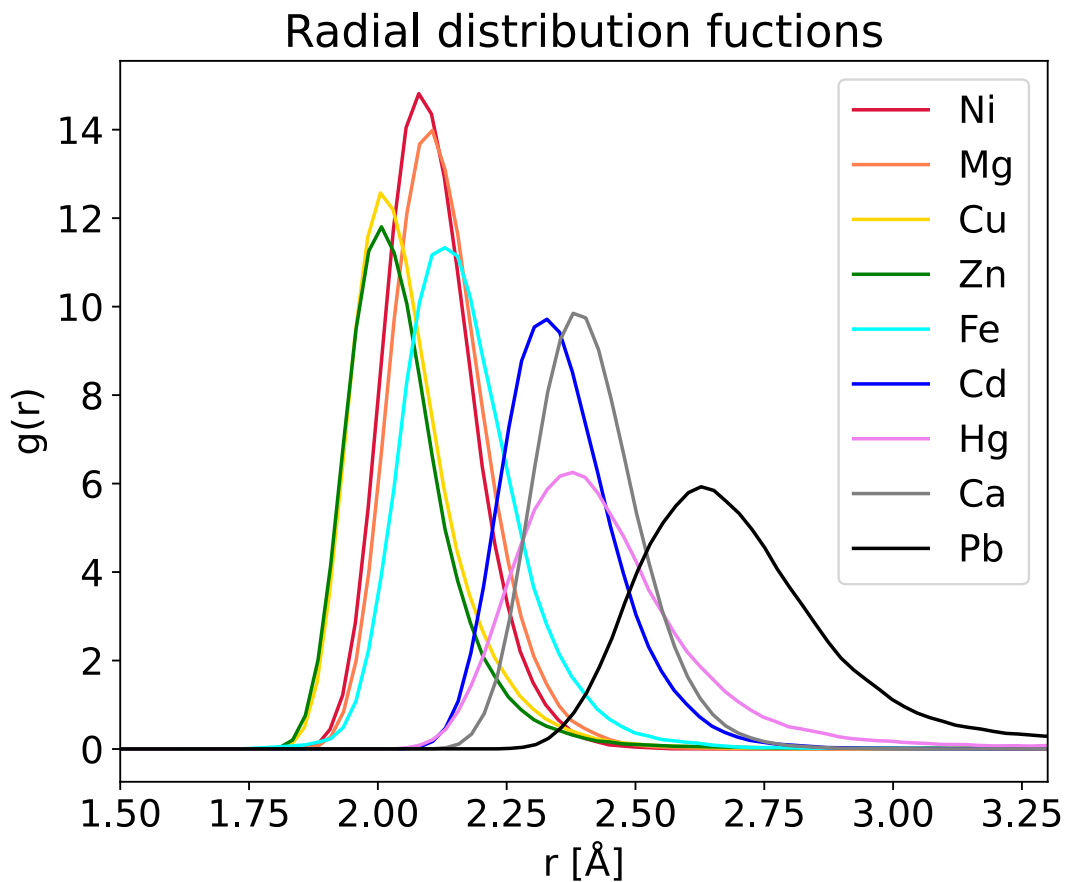

FIG. 2: The first peak of the metal-oxygen radial distribution functions in a box of 64 water molecules, obtained from AIMD simulations at the PBE-D3/TZV2P level. Metal ions are in the legend box ordered according to their ionic radii.

TABLE III: Comparison of M^{2+}–O distances obtained with DFT-D3//COSMO-RS, AIMD, and published experimental results. If there were multiple M^{2+}–O distances differing by more than 0.02 Å in the DFT-D3//COSMO-RS optimal structures, all of them are listed. AIMD distances were taken as RDF maximum, except for Cu^{2+}, where, thanks to its stable pyramidal configuration in AIMD, it is possible to list two distinct well-defined Cu^{2+}–O distances.

M^{2+}	$r_{\mathrm{DFT-D3//COSMO-RS}}$ [Å]	r_{AIMD} [Å]	$r_{\mathrm{Exp.}}$ [Å]
Ca^{2+}	2.351	2.378	2.39–2.46 [31]
Cd^{2+}	2.314	2.327	2.29 [8, 9]
Cu^{2+}	1.991, 2.216	2.026, 2,230	1.96, 2.24 [7]
Fe^{2+}	2.109, 2.129	2.128	2.070, 2.072 [7, 8]
Hg^{2+}	2.315, 2.347	2.376	2.33–3.08 [8, 9, 21]
Mg^{2+}	2.076	2.103	2.00-2.15 [7, 9]
Ni^{2+}	2.079	2.080	2.002 [8]
Pb^{2+}	2.387, 2.457, 2.491, 2.524, 2.601	2.626	2.31–2.81 [24, 25]
Zn^{2+}	2.110	2.004	2.057 [7, 8]

The integral of the first RDF peak up to the first RDF minimum (Fig. 3) gives the mean (time-averaged) coordination number of the first solvation shell. This again illustrates that some of the ions adopt multiple semi-stable coordination numbers, as the value of the integral of the RDF of the first peak is non-integer.
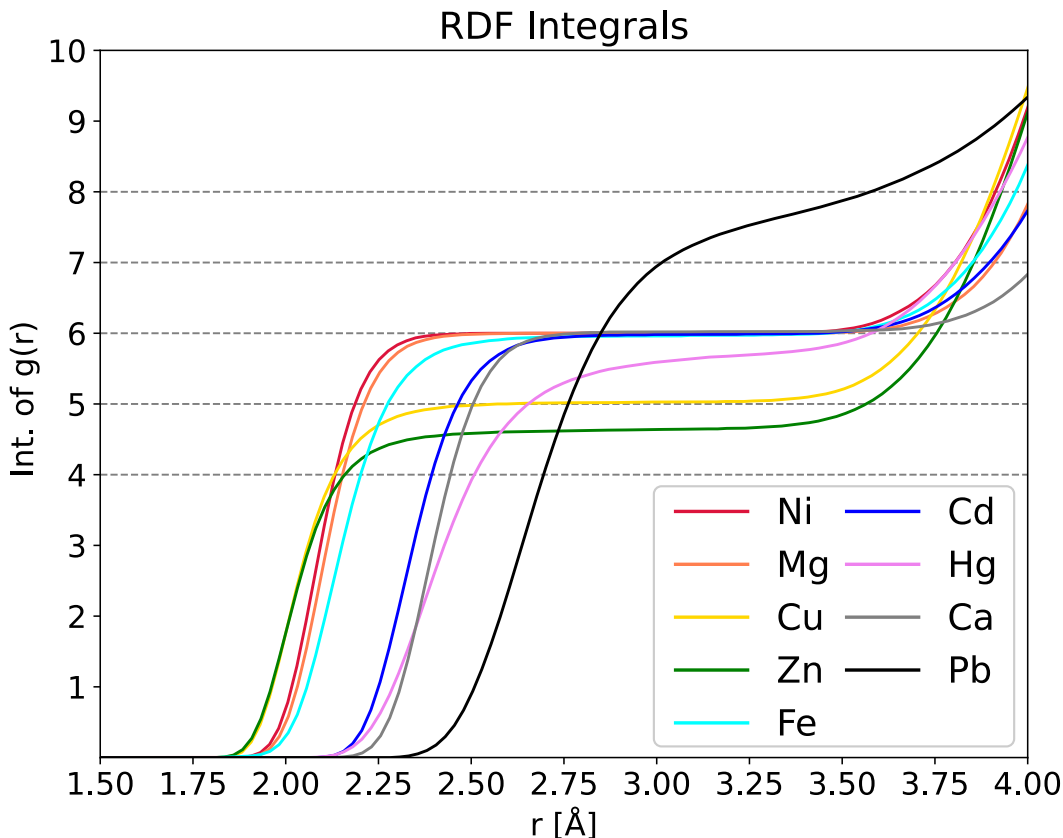
FIG. 3: Integrals of the M^{2+}–O radial distribution functions of metal ions in a box of 64 water molecules, calculated at PBE-D3/TZVPP level.

To discuss coordination numbers in more detail, we depicted their distribution over AIMD simulations for each ion in Fig. 4 together with the coordination number from DFT with implicit solvation (Fig. 1) and experimentally obtained coordination numbers. The geometries of such aqua ions (if known experimentally) are summarized in Table IV. Distributions of coordination numbers differ substantially for various ions. Both AIMD and DFT-D3//COSMO-RS coordination numbers are fully in line with the experimental results for Mg^{2+} and Fe^{2+}. Both of these ions are unambiguously reported to adopt regular octahedrons in water solution.[8, 9, 17, 18] For Ni^{2+}, both calculations and published experiments agree with coordination number 6 and clear regular octahedron,[8, 22, 23] whereas AIMD also shows a small fraction of five-coordination. Similarly, for Cd^{2+}, DFT-D3//COSMO-RS and AIMD both agree on CN 6, which is often reported, together with possible equilibrium with CN 7.[7, 32, 33]

Both AIMD and DFT-D3//COSMO-RS calculations also point to the coordination number of five for Cu^{2+}. Although older works have generally claimed 6-fold coordination,[60–67] it was shown that this actually may not be correct.[34] It is now believed that CN 5 is preferable due to the $3d^9$ electronic structure of Cu^{2+} atomic shell, which destabilizes the octahedral coordination via Jahn–Teller distortion. The 5-fold coordination was also reported by both AIMD and DFT calculations,[68, 69] suggesting an equilibrium between a tetragonal pyramid and trigonal bipyramid. Moreover, it was shown that X-ray experimental methods were unable to provide a clear answer,[70, 71] pointing out the potential pitfalls of these methods in cases where there may

10

coexist multiple stable coordinations.[15]

In the case of Hg^{2+}, the DFT-D3//COSMO-RS suggests both CN 5 and 6, as the corresponding ΔG_{HYD} between the two is as small as 0.1 kcal·mol^{-1}. Correspondingly, AIMD points to the equilibrium between these two coordination numbers as well. Published results are in line with this, mostly agreeing on CN 6 with the geometry of distorted octahedron,[19, 20] although the experimental and theoretical evidence for CN 7[21] has been reported as well.

Ca^{2+} is theoretically predicted to be a hexa-coordinated octahedron by both methods, However, the addition of the seventh water molecule is associated with ΔG of 1.1 kcal·mol^{-1} in DFT-D3//COSMO-RS, which suggests possibly stable hepta-coordination. Experimental results obtained from X-ray diffraction, neutron diffraction, and EXAFS are scattered over 6-fold, 7- and 8-fold coordination,[16, 26, 29–31] but 10 is reported as well,[29] illustrating that the question may be still open.

Zn^{2+} has been reported to prefer CN of 6 with waters in an octahedral coordination geometry. This conclusion has been obtained both from neutron diffraction and EXAFS experiments.[8, 22, 28] This is fully in line with our DFT-D3//COSMO-RS prediction. AIMD at PBE-D3/TZVPP level fails to predict the CN 6, pointing to the average CN 4.5 in contrast. We further investigated this obvious discrepancy by changing the DFT functional to BP86 and switching off the dispersion correction between Zn^{2+} and waters. However, this led to the CN 4 and tetrahedral coordination geometry for Zn^{2+} aqua complex (see SI, Fig. S1). The initial force field MD trajectories converged to the CN 6 as well. At the same time, there is by far the largest difference in the Zn^{2+}–O equilibrium distance between the DFT-D3//COSMO-RS and AIMD calculations. While tetrahedral complexes of Zn^{2+} are reported, those are composed of other ligands than water.[72] We conclude that this might be an error of the combination of the used effective core potential and basis. This is the only case where AIMD failed to reproduce what is now accepted as the correct Zn^{2+} coordination number.

For Pb^{2+}, the experimental results in the condensed phase are rather limited. There is an old NMR experiment[27] suggesting a coordination number of 6 and two more recent EXAFS studies,[24, 25] failing to determine the coordination number due to the very broad Pb^{2+}–O distance distribution, but inclining to hemi-directed structures with 5 to 7 water molecules in the first layer. Moreover, results from theoretical studies vary as well; in most cases, CN 6–8 are reported,[73, 74] but some simulations report CN 9 as well.[75] Results mostly agree that 6- and 7-fold hydrated structures are hemidirected, while 8-fold and larger CNs are holodirected.[73, 76] The size of the ECP plays a crucial role here because structures obtained with the smaller ECP are significantly less hemidirected.[73] Theoretical results are, therefore, shifted towards larger coordination numbers in comparison to (limited) experiments. One of the possible explanations is that experiments may fail to detect very long Pb^{2+}–O bonds.[74] All of this illustrates that the problem of Pb^{2+} hydration is far from being solved. Our AIMD results fit well in this context, showing mostly the equilibrium between seven and eight water molecules in the first solvation shell, where for CN 7, the hydration structure is hemidirected, and for CN 8 holodirected. There are also small fractions of CN 6 and 9. Contrary to that, DFT-D3//COSMO-RS prefers the hemidirected coordination with the CN 5, which is on the (very) low border of what has ever been reported, as discussed above. We consider this to be an error of the implicit solvent model suggesting that more than the first shell may be necessary for heavier atoms or those with a non-symmetric solvation shell. Pb^{2+} is the only ion where DFT-D3//COSMO-RS fails to predict the experimentally reported coordination number. However, it correctly predicted the change from hemi- to holo- hydration between CN 7 and 8 (although these have positive ΔG of hydration).
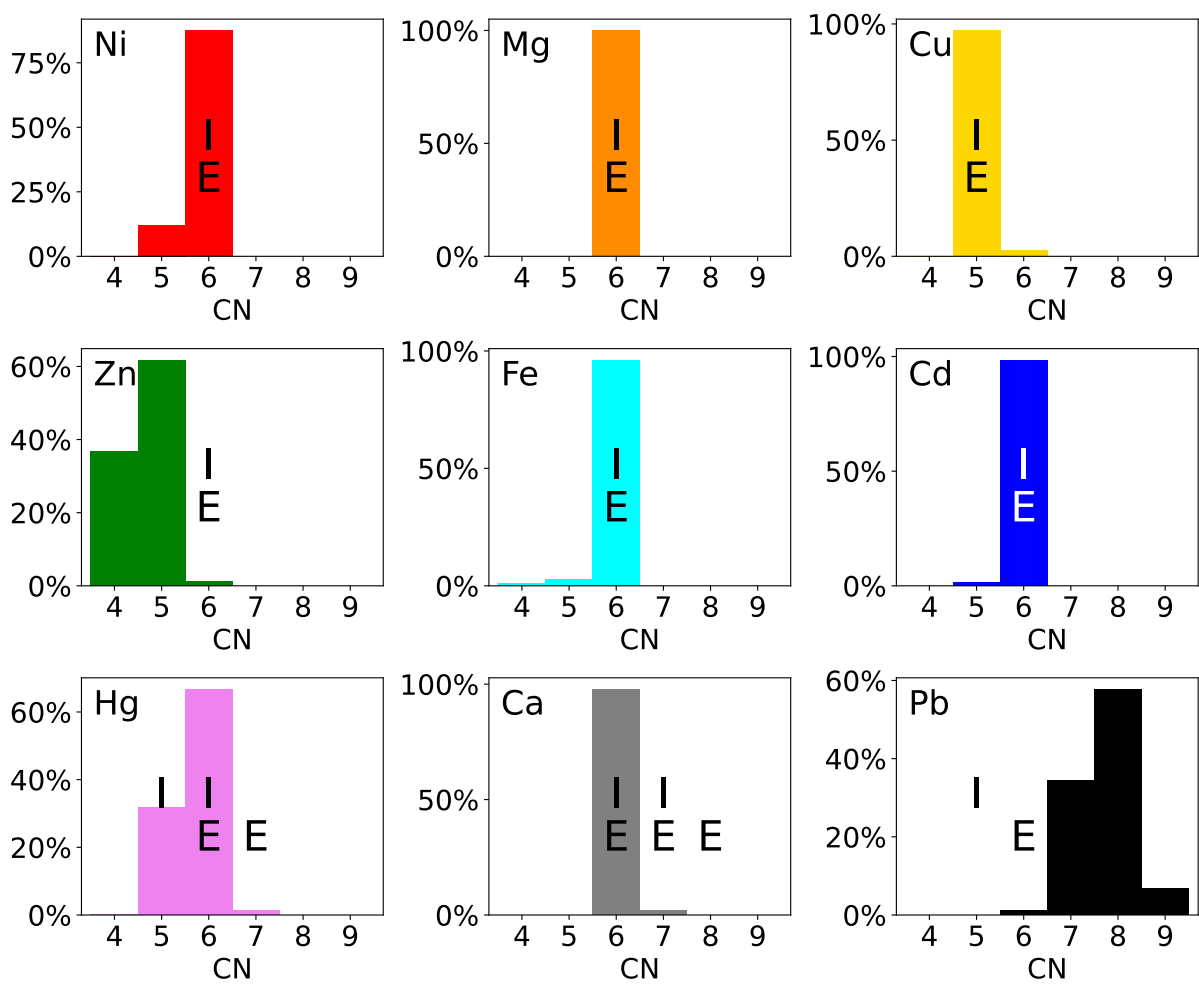
FIG. 4: Distribution of coordination numbers for metal ions in a box of 64 water molecules over all the AIMD trajectories. "I" denotes results in DFT-D3//COSMO-RS implicit solvent, "E" stands for experimentally reported values.

TABLE IV: Coordination numbers for metal aqua ions obtained from DFT at the BP86-D3//COSMO-RS level and AIMD PBE-D3/TZV2P level with 64 explicit water molecules, with the geometry of the aqua ion, together with experimentally obtained results from the literature, discussed in the text.

M^{2+}	COSMO-RS CN	COSMO-RS geom.	AIMD CN	AIMD geom.	Exp. CN	Exp. geom.
Ca^{2+} Irregular	6-7 6	Octahedron, Octahedron	$6–8^a$	Octahedron, Not determined		
Cd^{2+}	6	Octahedron	6	Octahedron	6–7	Octahedron
Cu^{2+}	5	Tetragonal pyramid	5	Tetragonal pyramid	5	Tetragonal pyramid
Fe^{2+}	6	Octahedron	6	Octahedron	6	Octahedron
Hg^{2+}	5–6	Trigonal bipyramid, Octahedron	5–6	Tetragonal pyramid, Octahedron	6–7	Octahedron, Irregular
Mg^{2+}	6	Octahedron	6	Octanhedron	6	Octahedron
Ni^{2+}	6	Octahedron	6	Octahedron	6	Octahedron
Pb^{2+}	5	Irregular	7–9	Irregular	$6^{b,c}$	Not determined
Zn^{2+}	6	Octahedron	4–5	Tetrahedron, Trigonal bipyramid	6	Octahedron

[a])There is also an experiment with CN 10,[29], but we consider it unreliable due to the significant difference in comparison with the ions with similar size and also with other experimental results for Ca^{2+}.
[b])The single one published experiment claims coordination number 6, two more experiments fail to determine it precisely but suggest CN 5–7.
[c])For Pb^{2+}, a significant amount of theoretical results do not agree with experimental ones, showing rather larger coordination numbers (6–9).

IV.   Conclusion

AIMD simulations of biologically relevant metal dications in bulk water and DFT calculations employing an implicit COSMO-RS solvent model were carried out. In the latter approach, sequential hydration was employed to determine the most stable aqua complexes of the ions. These were then compared with the distributions of aqua complexes from AIMD trajectories. Both types of calculations generally agree with each other as well as with published experimental results. However, there are two important exceptions. AIMD failed to reproduce the generally accepted octahedral hydration for Zn^{2+}, pointing rather to the tetrahedral coordination with CN 4 for both PBE

and BP86 functionals, whereas DFT-D3//COSMO-RS agrees with the experimental coordination number. The second exception is Pb^{2+}, for which DFT-D3//COSMO-RS calculations predicted a hemi-hydrated structure with CN 5. In contrast, AIMD calculations predict CN 7 and 8, in agreement with previous theoretical studies.

We conclude that the present conceptually simple and computationally efficient approach based on the COSMO-RS implicit solvent model combined with the DFT-D3 quantum chemical calculations with only the first explicit solvent shell is able to predict the correct coordination number for most of the investigated ions. However, in cases with a significantly non-symmetric solvent shell, the inclusion of an explicit second solvation shell may be necessary for a correct description.

Acknowledgement

Author declarations

Conflict of interest

The authors have no conflicts to disclose.

Author contributions

T. Kalvoda: Conceptualization (equal); Data curation (lead); Formal analysis (lead); Investigation (lead); Visualization (lead); Writing – original draft (equal). Tomas Martinek: Conceptualization (supporting); Data curation (equal); Formal analysis (equal); Visualization (supporting); Writing – original draft (equal); Writing – review & editing (supporting). P. Jungwirth: Conceptualization (equal); Methodology (equal); Funding acquisition (equal); Writing – review & editing (equal). L. Rulíšek: conceptualization (lead); Funding acquisition (equal); Methodology (equal); Supervision (lead); Visualization (supporting); Writing – review & editing (lead).

Data availability

The data that support the findings of this study are available within the article and its supplementary material (.pdf file with methodology details and .zip file with the raw AIMD and COSMO-RS data).

References

[1]M. Stillman, *Biological Inorganic Chemistry. Structure and Reactivity. Edited by Ivano Bertini, Harry B. Gray, Edward I. Stiefel and Joan S. Valentine.* (University Science Book, 2007).

[2]T. Dudev and C. Lim, "Metal Binding Affinity and Selectivity in Metalloproteins: Insights from Computational Studies", Annual Review of Biophysics **37**, 97–116 (2008).

[3]T. A. Mohammed, C. M. Meier, T. Kalvoda, M. Kalt, L. Rulíšek, and M. S. Shoshan, "Potent Cyclic Tetrapeptide for Lead Detoxification", Angewandte Chemie International Edition **60**, 12381–12385 (2021).

[4]L. Sauser, T. Kalvoda, A. Kavas, L. Rulíšek, and M. S. Shoshan, "Cyclic Octapeptides Composed of Two Glutathione Units Outperform the Monomer in Lead Detoxification", ChemMedChem **17**, e202200152 (2022).

[5]L. Sauser, T. A. Mohammed, T. Kalvoda, S.-J. Feng, B. Spingler, L. Rulíšek, and M. S. Shoshan, "Thiolation and Carboxylation of Glutathione Synergistically Enhance Its Lead-Detoxification Capabilities", Inorganic Chemistry **60**, 18620–18624 (2021).

[6]O. Gutten and L. Rulíšek, "Predicting the Stability Constants of Metal-Ion Complexes from First Principles", Inorganic Chemistry **52**, 10347–10355 (2013).

[7]I. Persson, "Structures of Hydrated Metal Ions in Solid State and Aqueous Solution", Liquids **2**, 210–242 (2022).

[8]H. Ohtaki and T. Radnai, "Structure and dynamics of hydrated ions", Chemical Reviews **93**, 1157–1204 (1993).

[9]G. Johansson, "Structures of Complexes in Solution Derived from X-Ray Diffraction Measurements", in *Advances in Inorganic Chemistry*, Vol. 39, edited by A. G. Sykes (Academic Press, Jan. 1992), pp. 159–232.

[10]E. A. Stern, D. E. Sayers, and F. W. Lytle, "Extended x-ray-absorption fine-structure technique. III. Determination of physical parameters", Physical Review B **11**, 4836–4846 (1975).

[11]G. W. Neilson, "Diffraction studies of aqueous electrolyte solutions", Pure and Applied Chemistry **60**, 1797–1806 (1988).

[12]E. Constable, J. A. McCleverty, and T. J. Meyer, *Comprehensive Coordination Chemistry II: From Biology to Nanotechnology*, 2nd edition (Elsevier Science, Amsterdam Boston, Dec. 2003).

[13]G. Bunker, *Introduction to XAFS: A Practical Guide to X-ray Absorption Fine Structure Spectroscopy* (Cambridge University Press, Cambridge, 2010).

[14]J. J. Rehr and R. C. Albers, "Theoretical approaches to x-ray absorption fine structure", Reviews of Modern Physics **72**, 621–654 (2000).

[15]J. Chaboy, A. Muñoz-Páez, P. J. Merkling, and E. Sánchez Marcos, "The hydration of Cu^{2+}: Can the Jahn-Teller effect be detected in liquid solution?", The Journal of Chemical Physics **124**, 064509 (2006).

[16]M. M. Probst, T. Radnai, K. Heinzinger, P. Bopp, and B. M. Rode, "Molecular dynamics and x-ray investigation of an aqueous calcium chloride solution", The Journal of Physical Chemistry **89**, 753–759 (1985).

[17]Y. Qing, C. Xing, Z. Jing, Z. Hai-Feng, Z. Wang-Sheng, Z. Xu-Sheng, A. Marcelli, and W. Zi-Yu, "Local hydrated structure of an Fe^{2+}/Fe^{3+} aqueous solution: an investigation using a combination of molecular dynamics and X-ray absorption fine structure methods", Chinese Physics C **37**, 038003 (2013).

[18]E. Kálmán, T. Radnai, G. Pálinkás, F. Hajdu, and A. Vértes, "Hydration of iron(II) ion in aqueous solutions", Electrochimica Acta **33**, 1223–1228 (1988).

[19]O. Sobolev, G. J. Cuello, G. Román-Ross, N. T. Skipper, and L. Charlet, "Hydration of Hg^{2+} in Aqueous Solution Studied by Neutron Diffraction with Isotopic Substitution", The Journal of Physical Chemistry A **111**, 5123–5125 (2007).

[20]A. T. Afaneh, G. Schreckenbach, and F. Wang, "Theoretical Study of the Formation of Mercury (Hg^{2+}) Complexes in Solution Using an Explicit Solvation Shell in Implicit Solvent Calculations", The Journal of Physical Chemistry B **118**, 11271–11283 (2014).

[21]G. Chillemi, G. Mancini, N. Sanna, V. Barone, S. Della Longa, M. Benfatto, N. V. Pavel, and P. D'Angelo, "Evidence for Sevenfold Coordination in the First Solvation Shell of Hg(II) Aqua Ion", Journal of the American Chemical Society **129**, 5430–5436 (2007).

[22]P. D'Angelo, V. Barone, G. Chillemi, N. Sanna, W. Meyer-Klaucke, and N. V. Pavel, "Hydrogen and Higher Shell Contributions in Zn^{2+}, Ni^{2+}, and Co^{2+} Aqueous Solutions: An X-ray Absorption Fine Structure and Molecular Dynamics Study", Journal of the American Chemical Society **124**, 1958–1967 (2002).

[23]G. W. Neilson, J. E. Enderby, and A. D. Buckingham, "The structure of an aqueous solution of nickel chloride", Proceedings of the Royal Society of London. A. Mathematical and Physical Sciences **390**, 353–371 (1997).

[24]I. Persson, K. Lyczko, D. Lundberg, L. Eriksson, and A. Płaczek, "Coordination Chemistry Study of Hydrated and Solvated Lead(II) Ions in Solution and Solid State", Inorganic Chemistry **50**, 1058–1072 (2011).

[25]J. R. Bargar, G. E. Brown, and G. A. Parks, "Surface complexation of Pb(II) at oxide-water interfaces: I. XAFS and bond-valence determination of mononuclear and polynuclear Pb(II) sorption products on aluminum oxides", Geochimica et Cosmochimica Acta **61**, 2617–2637 (1997).

[26]D. Spångberg, K. Hermansson, P. Lindqvist-Reis, F. Jalilehvand, M. Sandström, and I. Persson, "Model Extended X-ray Absorption Fine Structure (EXAFS) Spectra from Molecular Dynamics Data for Ca^{2+} and Al^{3+} Aqueous Solutions", The Journal of Physical Chemistry B **104**, 10467–10472 (2000).

[27]T. J. Swift and W. G. Sayre, "Determination of Hydration Numbers of Cations in Aqueous Solution by Means of Proton NMR", The Journal of Chemical Physics **44**, 3567–3574 (1966).

[28]V. Migliorati, G. Mancini, S. Tatoli, A. Zitolo, A. Filipponi, S. De Panfilis, A. Di Cicco, and P. D'Angelo, "Hydration Properties of the Zn^{2+} Ion in Water at High Pressure", Inorganic Chemistry **52**, 1141–1150 (2013).

[29]N. A. Hewish, G. W. Neilson, and J. E. Enderby, "Environment of Ca^{2+} ions in aqueous solvent", Nature **297**, 138–139 (1982).

[30]F. Jalilehvand, D. Spångberg, P. Lindqvist-Reis, K. Hermansson, I. Persson, and M. Sandström, "Hydration of the Calcium Ion. An EXAFS, Large-Angle X-ray Scattering, and Molecular Dynamics Simulation Study", Journal of the American Chemical Society **123**, 431–441 (2001).

[31]W. W. Rudolph and G. Irmer, "Hydration of the calcium(II) ion in an aqueous solution of common anions (ClO_4^-, Cl^-, Br^-, and NO_3^-)", Dalton Transactions **42**, 3919–3935 (2013).

[32]H. Kanno, "Nonexistence of Hydration Number Change of Cd^{2+} Ions in Aqueous $Cd(NO_3)_2$ Solution", Bulletin of the Chemical Society of Japan **59**, 3651–3652 (1986).

[33]P. D'Angelo, G. Chillemi, V. Barone, G. Mancini, N. Sanna, and I. Persson, "Experimental Evidence for a Variable First Coordination Shell of the Cadmium(II) Ion in Aqueous, Dimethyl Sulfoxide, and N,N'-Dimethylpropyleneurea Solution", The Journal of Physical Chemistry B **109**, 9178–9185 (2005).

[34]A. Pasquarello, I. Petri, P. S. Salmon, O. Parisel, R. Car, É. Tóth, D. H. Powell, H. E. Fischer, L. Helm, and A. E. Merbach, "First Solvation Shell of the Cu(II) Aqua Ion: Evidence for Fivefold Coordination", Science **291**, 856–859 (2001).

[35]T. Dudev, C. Grauffel, and C. Lim, "How Pb^{2+} Binds and Modulates Properties of Ca^{2+} – Signaling Proteins", Inorganic Chemistry **57**, Publisher: American Chemical Society, 14798–14809 (2018).

[36]R. A. Bernhoft, "Mercury Toxicity and Treatment: A Review of the Literature", Journal of Environmental and Public Health **2012**, e460508 (2011).

[37]Y. Marcus, "Thermodynamics of solvation of ions. Part 6. The standard partial molar volumes of aqueous ions at 298.15 K", Journal of the Chemical Society, Faraday Transactions **89**, 713–718 (1993).

[38]A. D. Mackerell Jr., M. Feig, and C. L. Brooks III, "Extending the treatment of backbone energetics in protein force fields: Limitations of gas-phase quantum mechanics in reproducing protein conformational distributions in molecular dynamics simulations", Journal of Computational Chemistry **25**, 1400–1415 (2004).

[39]H. J. C. Berendsen, J. R. Grigera, and T. P. Straatsma, "The missing term in effective pair potentials", The Journal of Physical Chemistry **91**, 6269–6271 (1987).

[40]S. Chatterjee, P. G. Debenedetti, F. H. Stillinger, and R. M. Lynden-Bell, "A computational investigation of thermodynamics, structure, dynamics and solvation behavior in modified water models", The Journal of Chemical Physics **128**, 124511 (2008).

[41]P. Li, B. P. Roberts, D. K. Chakravorty, and K. M. J. Merz, "Rational Design of Particle Mesh Ewald Compatible Lennard-Jones Parameters for +2 Metal Cations in Explicit Solvent", Journal of Chemical Theory and Computation **9**, 2733–2748 (2013).

[42]H. J. C. Berendsen, D. van der Spoel, and R. van Drunen, "GROMACS: A message-passing parallel molecular dynamics implementation", Computer Physics Communications **91**, 43–56 (1995).

[43]T. D. Kühne, M. Iannuzzi, M. Del Ben, V. V. Rybkin, P. Seewald, F. Stein, T. Laino, R. Z. Khaliullin, O. Schütt, F. Schiffmann, D. Golze, J. Wilhelm, S. Chulkov, M. H. Bani-Hashemian, V. Weber, U. Borštnik, M. Taillefumier, A. S. Jakobovits, A. Lazzaro, H. Pabst, T. Müller, R. Schade, M. Guidon, S. Andermatt, N. Holmberg, G. K. Schenter, A. Hehn, A. Bussy, F. Belleflamme, G. Tabacchi, A. Glöß, M. Lass, I. Bethune, C. J. Mundy, C. Plessl, M. Watkins, J. VandeVondele, M. Krack, and J. Hutter, "CP2K: An electronic structure and molecular dynamics software package - Quickstep: Efficient and accurate electronic structure calculations", The Journal of Chemical Physics **152**, 194103 (2020).

[44]J. P. Perdew, K. Burke, and M. Ernzerhof, "Generalized Gradient Approximation Made Simple", Physical Review Letters **78**, 1396–1396 (1996).

[45]S. Grimme, J. Antony, S. Ehrlich, and H. Krieg, "A consistent and accurate ab initio parametrization of density functional dispersion correction (DFT-D) for the 94 elements H–Pu", The Journal of Chemical Physics **132**, 154104 (2010).

[46] J. VandeVondele and J. Hutter, "Gaussian basis sets for accurate calculations on molecular systems in gas and condensed phases", The Journal of Chemical Physics **127**, 114105 (2007).

[47] S. Goedecker, M. Teter, and J. Hutter, "Separable dual-space Gaussian pseudopotentials", Physical Review B **54**, 1703–1710 (1996).

[48] G. Bussi, D. Donadio, and M. Parrinello, "Canonical sampling through velocity rescaling", The Journal of Chemical Physics **126**, 014101 (2007).

[49] A. D. Becke, "Density-functional exchange-energy approximation with correct asymptotic behavior", Physical Review A **38**, 3098–3100 (1988).

[50] J. P. Perdew, "Density-functional approximation for the correlation energy of the inhomogeneous electron gas", Physical Review B **33**, 8822–8824 (1986).

[51] S. Grimme, S. Ehrlich, and L. Goerigk, "Effect of the damping function in dispersion corrected density functional theory", Journal of Computational Chemistry **32**, 1456–1465 (2011).

[52] A. Klamt and G. Schüürmann, "COSMO: a new approach to dielectric screening in solvents with explicit expressions for the screening energy and its gradient", Journal of the Chemical Society, Perkin Transactions 2, 799–805 (1993).

[53] R. D. Shannon, "Revised effective ionic radii and systematic studies of interatomic distances in halides and chalcogenides", Acta Crystallographica Section A **32**, 751–767 (1976).

[54] *TURBOMOLE V7.6 2022, a development of University of Karlsruhe and Forschungszentrum Karlsruhe GmbH, 1989-2007, TURBOMOLE GmbH, since 2007; available from* `http://www.turbomole.com`.

[55] A. Klamt, "Conductor-like Screening Model for Real Solvents: A New Approach to the Quantitative Calculation of Solvation Phenomena", The Journal of Physical Chemistry **99**, 2224–2235 (1995).

[56] A. Klamt, V. Jonas, T. Bürger, and J. C. W. Lohrenz, "Refinement and Parametrization of COSMO-RS", The Journal of Physical Chemistry A **102**, 5074–5085 (1998).

[57] F. Eckert and A. Klamt, "Fast solvent screening via quantum chemistry: COSMO-RS approach", AIChE Journal **48**, 369–385 (2002).

[58] A. Klamt and M. Diedenhofen, "A refined cavity construction algorithm for the conductor-like screening model", Journal of Computational Chemistry **39**, 1648–1655 (2018).

[59] V. Kostal, P. E. Mason, H. Martinez-Seara, and P. Jungwirth, "Common Cations Are Not Polarizable: Effects of Dispersion Correction on Hydration Structures from Ab Initio Molecular Dynamics", The Journal of Physical Chemistry Letters **14**, 4403–4408 (2023).

[60] H. Ohtaki and M. Maeda, "An X-Ray Diffraction Study of the Structure of Hydrated Copper(II) Ion in a Copper(II) Perchlorate Solution", Bulletin of the Chemical Society of Japan **47**, 2197–2199 (1974).

[61] M. Magini, "Coordination of copper(II). Evidence of the Jahn–Teller effect in aqueous perchlorate solutions", Inorganic Chemistry **21**, 1535–1538 (1982).

[62] J. Garcia, M. Benfatto, C. R. Natoli, A. Bianconi, A. Fontaine, and H. Tolentino, "The quantitative Jahn-teller distortion of the Cu^{2+} site in aqueous solution by xanes spectroscopy", Chemical Physics **132**, 295–302 (1989).

[63]G. Licheri, A. Musinu, G. Paschina, G. Piccaluga, G. Pinna, and A. F. Sedda, "Coordination of Cu(II) in $Cu(NO_3)_2$ aqueous solutions", The Journal of Chemical Physics **80**, 5308–5311 (1984).

[64]Y. Tajiri and H. Wakita, "An EXAFS Investigation of the Coordination Structure of Copper(II) Ions in Aqueous $Cu(ClO_4)_2$ and Methanolic $CuCl_2$ Solutions", Bulletin of the Chemical Society of Japan **59**, 2285–2291 (1986).

[65]T. K. Sham, J. B. Hastings, and M. L. Perlman, "Application of the EXAFS method to Jahn—Teller ions: static and dynamic behavior of $Cu(H_2O)_6{}^{2+}$ and $Cr(H_2O)_6{}^{2+}$ in aqueous solution", Chemical Physics Letters **83**, 391–396 (1981).

[66]B. Beagley, A. Eriksson, J. Lindgren, I. Persson, L. G. M. Pettersson, M. Sandstrom, U. Wahlgren, and E. W. White, "A computational and experimental study on the Jahn-Teller effect in the hydrated copper (II) ion. Comparisons with hydrated nickel (II) ions in aqueous solution and solid Tutton's salts", Journal of Physics: Condensed Matter **1**, 2395 (1989).

[67]S. E. Okan and P. S. Salmon, "The Jahn-Teller effect in solutions of flexible molecules: a neutron diffraction study on the structure of a Cu^{2+} solution in ethylene glycol", Molecular Physics **85**, 981–998 (1995).

[68]J. V. Burda, M. Pavelka, and M. Šimánek, "Theoretical model of copper Cu(I)/Cu(II) hydration. DFT and ab initio quantum chemical study", Journal of Molecular Structure: THEOCHEM **683**, 183–193 (2004).

[69]X. Liu, X. Lu, E. J. Meijer, and R. Wang, "Hydration mechanisms of Cu^{2+}: tetra-, penta- or hexa-coordinated?", Physical Chemistry Chemical Physics **12**, 10801–10804 (2010).

[70]M. Benfatto, P. D'Angelo, S. Della Longa, and N. V. Pavel, "Evidence of distorted fivefold coordination of the Cu^{2+} aqua ion from an x-ray-absorption spectroscopy quantitative analysis", Physical Review B **65**, 174205 (2002).

[71]P. Frank, M. Benfatto, R. K. Szilagyi, P. D'Angelo, S. Della Longa, and K. O. Hodgson, "The Solution Structure of $[Cu(aq)]^{2+}$ and Its Implications for Rack-Induced Bonding in Blue Copper Protein Active Sites", Inorganic Chemistry **44**, 1922–1933 (2005).

[72]V. Patel, S.-L. Dahlroth, V. Rajakannan, H. T. Ho, T. Cornvik, and P. Nordlund, "Structure of the C-Terminal Domain of the Multifunctional ICP27 Protein from Herpes Simplex Virus 1", Journal of Virology **89**, 8828–8839 (2015).

[73]M. C. F. Wander and A. E. Clark, "Hydration Properties of Aqueous Pb(II) Ion", Inorganic Chemistry **47**, 8233–8241 (2008).

[74]C. Gourlaouen, H. Gérard, and O. Parisel, "Exploring the Hydration of Pb^{2+}: Ab Initio Studies and First-Principles Molecular Dynamics", Chemistry – A European Journal **12**, 5024–5032 (2006).

[75]T. S. Hofer and B. M. Rode, "The solvation structure of Pb(II) in dilute aqueous solution: An ab initio quantum mechanical/molecular mechanical molecular dynamics approach", The Journal of Chemical Physics **121**, 6406–6411 (2004).

[76]A. M. Kuznetsov, A. N. Masliy, and G. V. Korshin, "Quantum-chemical simulations of the hydration of Pb(II) ion: structure, hydration energies, and pK_{a1} value", Journal of Molecular Modeling **24**, 193 (2018).